



# Direct statistical comparison of hydrodynamic mixing experiments and simulations

W. Rider<sup>1</sup>, J. Kamm<sup>1</sup>, P. Rightley<sup>1</sup>, K. Prestridge<sup>1</sup>,  
R. Benjamin<sup>1</sup>, P. Vorobieff<sup>2</sup>

<sup>1</sup>*Los Alamos National Laboratory, Los Alamos, USA*

<sup>2</sup>*University of New Mexico, Albuquerque, USA*

## Abstract

Fluid mixing phenomena are dominated by irregular structures induced by flow instabilities, which lead to non-deterministic behavior. Hence, there is no direct, pointwise method to establish the correspondence between experimental data and numerical simulation. Using statistical analysis methods, we examine the correspondence between experimental data and simulations. We examine the detailed structures of mixing experiments and their simulation for the Richtmyer-Meshkov (RM) instability. To examine the compressible RM instability, we use the gas curtain experiment of Rightley et al. [8]. Numerical simulations of both experimental configurations were conducted with a variety of flow codes. The experiment and simulation agree at the scale of the mixing zone width, there is statistically significant disagreement at smaller scales. We hypothesize that subgrid-scale physics and/or details of the numerical integration may explain these differences.

## 1 Introduction

Comparison of numerical simulation results with experimental data provides an essential element in the evaluation of modeling capabilities. Ideally, in such an evaluation both numerical and experimental values are examined in an identical manner. This is precisely the course we have taken in recent years in our examination of the gas curtain experiment, the results of which [3] have raised more questions than they have answered. The gas

curtain Richtmyer-Meshkov experiment of Rightley *et al.* ([8, 10, 9]) involves shocking a curtain of SF<sub>6</sub> with a Mach 1.2 shockwave and examining the subsequent fluid mixing driven by the deposition of baroclinic vorticity in the gas curtain. The baroclinic vorticity arises due to a mismatch between density and pressure gradients, which, as a vorticity source, can act to enhance mixing in the flow. The experiments and our comparative are detailed in a companion paper at this conference [4].

Hydrodynamic flow fields can be crudely categorized into two basic regimes. The first is deterministic or “ordered” flow fields, for which a unique solution can be obtained (*e.g.*, laminar flow). The second is non-deterministic or “disordered” flow fields, for which a unique solution cannot be expected (*e.g.*, turbulent flow). Hydrodynamic mixing (in general) and the gas curtain experiment (in particular) fall into the latter category, *i.e.*, a unique solution cannot be expected at any but the very earliest times. Our ultimate goal is to answer the question: “Above what scale can we trust the fidelity of a computational simulation of mixing phenomena?”

In response to this issue, the best to be hoped for in such cases is that the simulation faithfully reproduce the “large scales.” Additionally, it is devoutly to be desired that one have some justifiable notion of which scales are resolved and which are not. For scientifically meaningful simulation of such situations, therefore, one must address and quantify the statistical nature of mixing as well as the variation of the flow phenomena with length scale. There are no universally accepted measures of these properties. In the present work, we shall focus on the fractal dimension, and quote results for wavelet and Fourier analyses as well as comparisons with experimentally obtained velocity fields.

In the present investigation, we simulate the gas curtain experiment primarily with the research code CUERVO [7], which uses a Godunov-type method in solving the Eulerian hydrodynamics equations. The question we address in the present work is, “How do different numerical methods affect the quantitative analysis of the gas curtain results?” Employing analysis techniques that are modifications of those used in previous investigations, we find that there are notable variations in the spectral signatures of different numerical methods on the gas curtain simulations. We obtain the reassuring result that different high-resolution shock capturing schemes all behave in a quantitatively similar fashion. We also present the disturbing finding that first-order schemes behave in a manner that is both

- *qualitatively* similar to the experimental data and
- *quantitatively* closer to the experiment than the (presumably “better”) high resolution methods.

In closing, we speculate as to some possible reasons behind these puzzling results and test some measures to mitigate the poor results.

## 2 The gas curtain Richtmyer-Meshkov experiment and analysis

In this section, we briefly review the gas curtain Richtmyer-Meshkov experiment. The interested reader is referred to the work of Rightley *et al.* [8, 10, 9] for further information. The experiments use a Mach 1.2 planar shock. In the test section, a vertical curtain of SF<sub>6</sub> is injected through a nozzle in the top, and removed through an exhaust plenum at the bottom. The evolving flow is imaged by a horizontal laser light sheet. A tracer material consisting of glycol fog is added to the curtain to greatly improve the dynamic range of the images, which are captured by CCD camera.

Previous work has established the ability to compute the development of the integral scale (*i.e.*, mixing layer width) for the gas curtain [1]. Unfortunately, the fidelity of the experimental data at that time was insufficient to determine the capacity of the numerical methods to compute sub-integral scales. More recent gas curtain experiments have a significantly higher experimental fidelity that does allow interrogation of scales smaller than the integral scale. Additionally, new experiments [5] include particle image velocimetry (PIV) of a simplified cylindrical initial condition, the validation of which is ongoing [6]. Later, we will relate the results of the PIV investigation to our current results.

As mentioned earlier, there are no universally accepted measures by which to compare details of disordered flow fields. The primary metric we consider herein is the local fractal dimension of the flowfield. The behavior of this measure, either between experimental observations and calculated results or among sets of calculated results, can be quantitatively compared over some range of length scales. We compute the fractal dimension using the variation method [2]. This local fractal dimension is the log-log slope of each pairwise set of data, as opposed to the best fit of the log-log slope over the entire scale range. For the case at hand, the local (variation) fractal dimension is calculated as the log-log slope between each pair of {scaled length, integrated variation} values. The outcome of this method is a plot in which the abscissa is the local length scale and the ordinate is the log-log slope between continuous pairs of {scaled length, integrated variation} values. This approach is the measure with which we quantify both experimental and computational data in section 4.

## 3 Numerical simulations

We use the images of the experimental initial conditions to initialize the computations. These images are corrected for noise by using a speckle filter that has a threshold intensity value equal to that of the CCD camera; the denoised images are used in the analysis of the experimental data. The denoised initial condition is subsequently smoothed with a Gaussian filter.



## 202 *Computational Methods and Experimental Measures*

These smoothed data are interpolated onto the computational grid, with the initial computational zone size approximately equal to the pixel size of the image.

Our computations are done primarily with two hydrocodes: RAGE, an adaptive grid Godunov method [1], and CUERVO, a Godunov code for investigating more advanced algorithms [7]. Both codes nominally solve the Euler equations of compressible flow. We chose to perform simulations with two different Euler codes, to see if the different algorithms in these codes (briefly described below) had a notable effect on either the gross or statistical characteristics of the computed mixing flow. Neither of these codes includes explicitly modeled viscous terms; however, preliminary simulations with equations containing viscous terms indicates no substantial difference in the computed results.

RAGE is a high resolution Godunov code. The Godunov method is operator split and implemented in a Lagrange-remap fashion with a linearized two-shock Riemann solver. The code has genuine multimaterial capability although the fluids have local thermal, pressure, and momentum equilibrium enforced. Boundary condition treatments are also limited; in this study we have imposed reflective boundaries at the top and bottom of the computational domain. RAGE also has an adaptive mesh refinement (AMR) feature, which we have employed to allow the smallest computational zones to decrease to one-half the linear dimension of the initial condition, *i.e.*, to one-half of the experimental pixel resolution. The code output is interpolated onto a mesh with resolution identical to that of the experimental images. RAGE is also capable of effectively utilizing the most modern computing resources available.

CUERVO is a single material research code. The principle role of CUERVO is to investigate advanced numerical integration techniques. At present, it uses unsplit differencing (both spatial and temporal) and an adaptive quadratic two-shock Riemann solver [7]. The treatment of boundary conditions is quite general and can be modified with ease. CUERVO does not presently have genuine multimaterial capability. Additionally, other physics can be added to the code without difficulty, a case in point being the diffusive terms (or, *e.g.*, simple turbulence models).

## 4 Results and analysis

We examine numerical simulations of a single gas curtain experiment, and use an image of the experimental initial conditions to initialize the computations. These images are corrected for noise by using a speckle filter that has a threshold intensity value equal to that of the CCD camera; the denoised images are used in the analysis of the experimental data. The denoised initial condition is subsequently smoothed with a Gaussian filter, which diffuses the initial values in a physically reasonable fashion. These smoothed

data are then interpolated onto the discrete computational grid. Figure 1 shows the results presented previously using the box counting method. The chief complication in this case is the arbitrary selection of contours. Given the poor comparison it is essential that this analysis be done in an unambiguously unbiased manner.

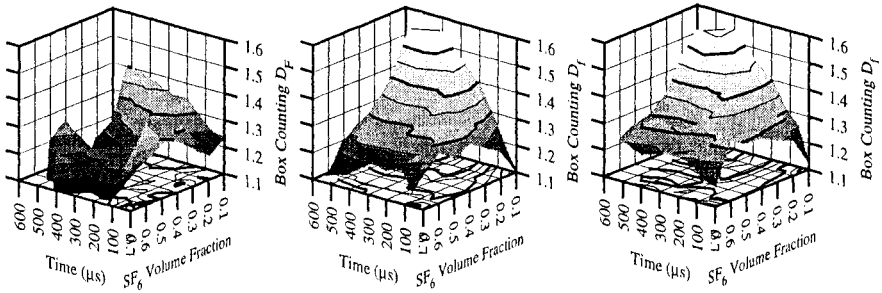


Figure 1: Box counting fractal dimension as a function of SF6 volume fraction and time for the gas curtain experiment (left), a RAGE calculation (middle), and a CUERVO calculation (right).

We show in Fig. 2 the local (variation) fractal dimension as a function of length scale for the experimental data at  $t=400 \mu\text{s}$  and two high-resolution data calculations, one on a  $200 \times 200$  grid and one on a  $400 \times 400$  grid. These results show a clear difference, at all scales, of this measure. The two computed results exhibit quantitative and qualitative similarity; additionally, the computed results appear to not converge to the experimental result with increased resolution.

To see if the behavior exhibited in Fig. 2 was in some way connected with the CUERVO code, we next considered results for the same initial conditions as calculated by a completely different code. Tariq Aslam of LANL kindly agreed to run this problem on a research code he wrote that uses a fifth-order WENO method (with third-order time integration). Figure 3 contains a plot comparing the  $t=400 \mu\text{s}$  local fractal dimension as a function of length scale for the experiment, the  $200 \times 200$  third-order CUERVO calculation, and the  $200 \times 200$  WENO calculation. Again, the high-resolution code values are both qualitatively and quantitatively similar, and differ significantly from the experimental results.

From these results, we hypothesized that some aspect of the high-resolution methods may be introducing extraneous high-frequency information in the simulations. Therefore, we performed a series of calculations in which the integrator was first-order accurate. The local fractal dimension results for that investigation are shown in Fig. 4 The plot at the left reveals the first-order results to bear both qualitative and quantitative similarity to that of the experiment.

We provide in Fig. 5 a comparison of the local fractal dimension of the

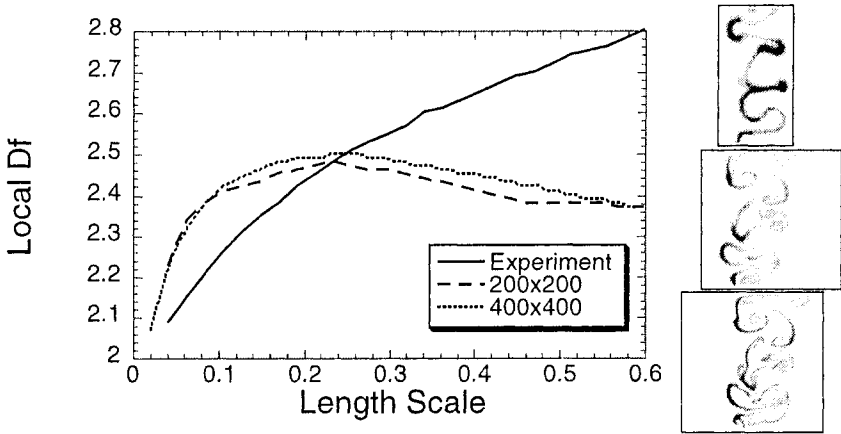


Figure 2: Local fractal (variation) dimension at  $t=400 \mu\text{s}$  of the experiment (solid), and second-order CUERVO calculations on  $200 \times 200$  (long dash) and  $400 \times 400$  (dotted) grids, all as functions of length scale. The corresponding volume fractions are on the right ordered as in the plot's legend.

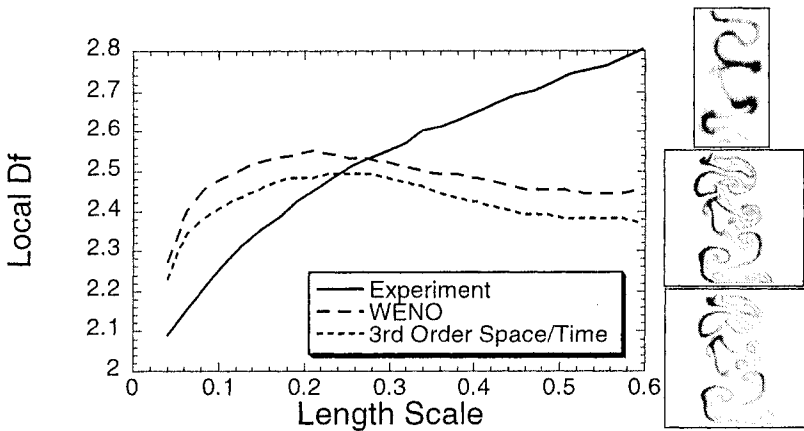


Figure 3: Local fractal dimension at  $t=400 \mu\text{s}$  of the experiment (solid),  $200 \times 200$  third-order CUERVO calculation (dotted), and  $200 \times 200$  WENO calculation (long dash) as a function of length scale. The corresponding volume fractions are on the right ordered as in the plot's legend.

experiment, the first-order, and second-order CUERVO calculations, both on  $400 \times 400$  grids. This figure clearly exhibits the qualitatively and quantitatively superior results provided by the first-order method. These results beg the question, "Does the improved correspondence between the experiment and first-order calculations relative to the second-order calculations hold up

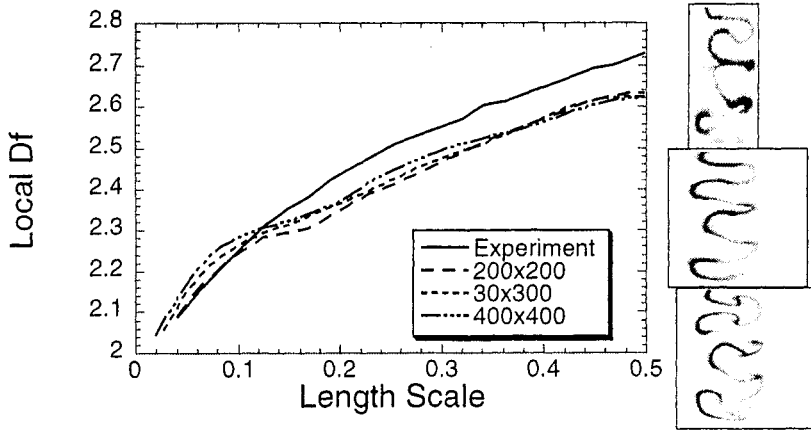


Figure 4: Local fractal dimension at  $t=400 \mu\text{s}$  of the experiment (solid), and first-order CUERVO calculations on  $200 \times 200$  (long dash),  $300 \times 300$  (dotted), and  $400 \times 400$  (dash-dot) grids, all functions of length scale. Corresponding volume fractions are on the right.

in different metrics?"

The PIV data recently available provides an entirely different basis for comparison. A PDF of the velocity field in the SF6 has a distribution that peaks at  $5 \text{ m/s}$  with a maximum velocity on the order of  $10 \text{ m/s}$ . The second-order computations have access to a more extensive velocity field with peak velocities more than five times larger. The second-order computational PDF of velocity has a peak greater than  $5 \text{ m/s}$ , but has large velocities on the order of  $70 \text{ m/s}$ . In contrast the first-order method's PDF for velocity peaks at less than  $5 \text{ m/s}$  in the SF6 and has maximum velocities near  $20 \text{ m/s}$ . Again the maximum velocities are larger, but this may be more reflective of the larger sample available in the calculations.

We address this question further by considering both Fourier and continuous wavelet analyses of the  $t=400 \mu\text{s}$  volume fractions. The Fourier spectrum is computed as the absolute-wavenumber derivative of the cumulative wavenumber (volume-fraction) spectral "energy." The continuous wavelet analysis uses the isotropic Marr ("Mexican hat") wavelet in two dimensions. We show in Fig. 6 the cumulative Fourier (volume-fraction) spectral energy, the corresponding Fourier density energy spectrum, and the Farge wavelet energy spectrum for the  $t=400 \mu\text{s}$  volume fractions shown in Fig. 5. The cumulative Fourier spectral energy shows a similar trend between the experiment and the first-order results, while the corresponding spectrum (i.e., the absolute-wavenumber derivative) largely eliminates the details. The wavelet energy spectrum exhibits both qualitative and quantitative similarity between the experiment and first-order results, over a range of scales, which are distinguished from the second-order results.

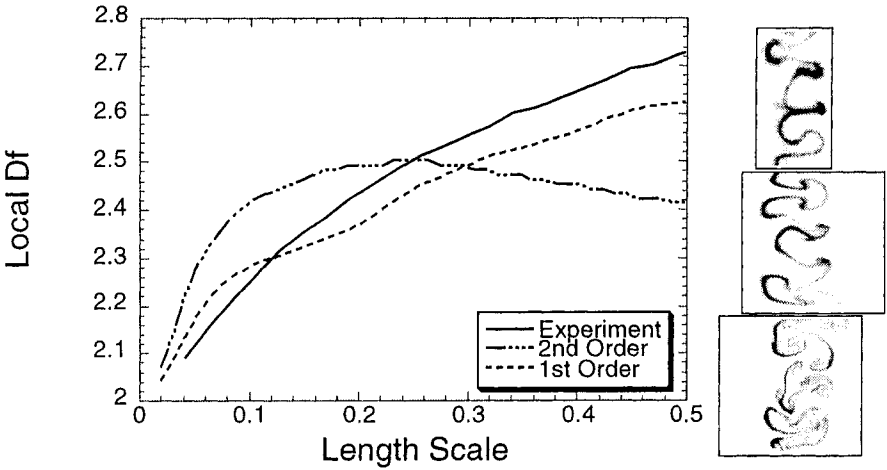


Figure 5: Local fractal dimension at  $t=400 \mu\text{s}$  of the experiment (solid), first-order CUERVO calculations on  $400 \times 400$  grid (dotted), and second-order CUERVO calculations on  $400 \times 400$  grid (dash-dot) grids. Corresponding volume fractions are on the right ordered as in the plot's legend.

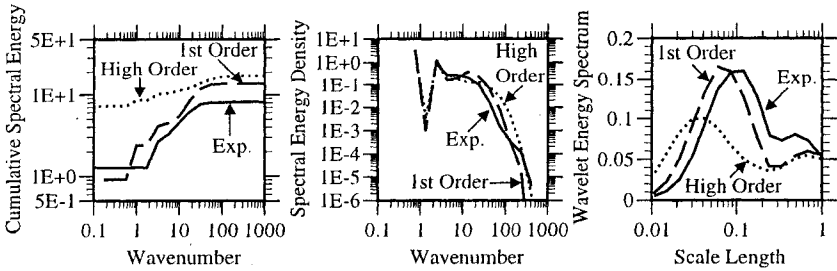


Figure 6: Cumulative Fourier spectral energy (left), Fourier energy density spectrum (middle), and wavelet energy spectrum (right) at  $t=400 \mu\text{s}$  for the experiment, first-order CUERVO calculations on  $200 \times 200$  grid, and the high-order WENO calculations on  $200 \times 200$  grid grids.

## 5 Summary

We have examined the gas curtain Richtmyer-Meshkov experiment of [8, 10, 9] and numerical simulations of that experiment using a modified scale-dependent fractal dimension measure. We find significant variations in the spectral signatures of different numerical methods on the gas curtain simulations. Different high-resolution shock capturing schemes exhibit quantitatively similar behavior; these results vary from first-order results, which are qualitatively similar to the experimental data and quantitatively closer





to the experiment than those of the (ostensibly “better”) high resolution methods. Continuous wavelet analysis provides independent confirmation of these trends. Perhaps as compellingly, recently available PIV data strongly supports the superiority of the first-order methods as compared with the high-order alternatives.

We speculate that some currently unknown aspects of high-resolution methods for multidimensional compressible flow may be undermining the statistical scaling in the gas-curtain Richtmyer-Meshkov simulations. A more tenuous albeit enticing conjecture is that these effects may be exacerbated in the low Mach number regime. Lastly, we observe that experiments with high fidelity diagnostics were critical to uncovering these issues. We would be delighted to have flow diagnostics of even higher spatial resolution. We shall further pursue our own efforts at rigorous validation exercises, and argue that quantitative “apples to apples” comparisons of experimental data with numerical results provide the most meaningful and compelling measure of the capabilities of numerical simulation.

Lastly, our results are not meant to imply that high-order methods should not be used. Rather, our viewpoint is that the high-order methods at present are not suitable for calculations of these experiments and must be modified to improve results. The most troubling aspect of the poor results is the lack of agreement in the large scales. Our most modest expectations include some sort of good comparison at the larger scales. This would seem to indicate that the methods are failing to compute the acoustic waves in a manner consistent with the experiments. Present work is focused on modifying the methods to better compute the acoustic waves. These modifications must be guided to a large extent by the performance of the methods on experiments.

## Acknowledgement

This work is available as report LA-UR-01-482, and was performed at Los Alamos National Laboratory, which is operated by the University of California for the United States Department of Energy under contract W-7405-ENG-36.

## References

- [1] R. M. Baltrusaitis, M. L. Gittings, R. P. Weaver, R. F. Benjamin & J. M. Budzinski, Simulation of Shock Generated Instabilities, *Phys. Fluids*, **8**, pp. 2471–2493, 1996.
- [2] Dubuc, B., Zucker, S.W., Tricot C., Quiniou, J.F., and Wehbi, D., “Evaluating the fractal dimension of surfaces”, *Proc. Roy. Soc. Lond. A*, **425** (1868), pp. 113–127, 1989b.



- [3] Kamm, J.R., Rider, W.J., Vorobieff, P., Rightley, P.M., Benjamin, R.F., and Prestridge, K.P., "Comparing the Fidelity of Numerical Simulations of Shock Generated Instabilities", in *Proceedings of the 22nd International Symposium on Shock Waves*, Ball, G.J., Hillier, R. and Roberts, G.T., eds., University of Southampton, pp. 683-688, 1999a. National Laboratory, Los Alamos, NM, LA-UR-98-3872, 1998.
- [4] Kamm, J., Rider, W., Rightley, P., Prestridge, K., Benjamin, R., and Vorobieff, P., "The Gas Curtain Experimental Technique and Analysis Methodologies" This Volume.
- [5] Prestridge K., Vorobieff, P., Rightley, P.M., and Benjamin, R.F., "Validation of an instability growth model using particle image velocimetry measurements," *Phys. Rev. Lett.*, **84**, pp. 4353-4356, 2000a.
- [6] Prestridge K., Zoldi, C., Vorobieff, P., Rightley, P.M., and Benjamin, R.F., Experiments and simulations of instabilities in a shock-accelerated gas cylinder, Los Alamos National Laboratory report LA-UR-00-3973, to be submitted to *Phys. Fluids*, 2000b.
- [7] W. J. Rider, An Adaptive Riemann Solver Using a Two-Shock Approximation, *Comp. Fluids*, **28**, pp. 741-777, 1999.
- [8] P. M. Rightley, P. Vorobieff & R. F. Benjamin, Evolution of a Shock Accelerated Thin Fluid Layer, *Phys. Fluids*, **9**, pp. 1770-1783, 1997.
- [9] P. M. Rightley, P. Vorobieff, R. Martin & R. F. Benjamin, Experimental Observations of the Mixing Transition in a Shock-accelerated Gas Curtain, *Phys. Fluids*, **11**, pp. 186-200, 1999.
- [10] P. Vorobieff, P. M. Rightley & R. F. Benjamin, Power-law Spectra of Incipient Gas-Curtain Turbulence, *Phys. Rev. Lett.*, **81**, pp. 2240-2243, 1998.